CONEM 2016
CONGRESSO NACIONAL DE ENGENHARIA MECÂNICA
21 - 25 AGOSTO DE 2016
FORTALEZA - CEARÁ

A THREE-DIMENSIONAL CONSTITUTIVE MODEL FOR TRANSFORMATION INDUCED PLASTICITY IN SHAPE MEMORY ALLOYS

Vanderson M. Dornelas, vandersonmarcio@yahoo.com.br[1]
Marcelo A. Savi, savi@mecanica.ufrj.br[1]
Sergio de A. Oliveira, amserol@yahoo.com.br[2]
Pedro Manuel C. L. Pacheco, calas@cefet-rj.br[2]
Alberto Paiva, paiva@puvr.uff.br[3]

[1]Universidade Federal do Rio de Janeiro
COPPE- Department of Mechanical Engineering, Center for Nonlinear Mechanics
21.941.972 - Rio de Janeiro - RJ - Brazil
[2]CEFET/RJ - Centro Federal de Educação Tecnológica Celso Suckow da Fonseca
Department of Mechanical Engineering, 20.271.110 - Rio de Janeiro - RJ - Brazil
[3]Universidade Federal Fluminense
Escola de Engenharia Industrial e Metalúrgica de Volta Redonda, 27.255.250- Volta Redonda - RJ - Brazil

Abstract: *Transformation induced plasticity (TRIP) is defined as the plastic flow arising from solid phase transformation processes involving volume and/or shape changes within the yield surface. This phenomenon occurs in shape memory alloys (SMAs) having significant influence over their macroscopic thermomechanical behavior. The present contribution presents a macroscopic three-dimensional constitutive model with internal constraints to describe the thermomechanical behavior of SMAs including classical and transformation induced plasticities. Comparisons between numerical and experimental results attest the model's ability to capture TRIP phenomenon.*

Keywords: Shape memory alloys, plasticity, transformation induced plasticity, constitutive model, numerical simulations.

1. INTRODUCTION

Shape memory alloys (SMAs) belong to the class of smart materials that have complex thermomechanical behavior related to different physical phenomena. Basically, the coupling between different fields establishes the remarkable properties of SMAs. Among the main behaviors, shape memory effect should be highlighted where the specimen can recover its original shape by the imposition of a proper thermomechanical loading process. Pseudoelasticity or superelasticity, two-way shape memory effect, phase transformation due to temperature variation, internal subloops due to incomplete phase transformation, and tension-compression asymmetry are other important behaviors identified on SMAs (Lagoudas, 2008; Paiva and Savi, 2006).

Plastic behavior of SMAs can be classified in two different behaviors: classical plasticity and transformation induced plasticity (TRIP). The classical plasticity arises from applied stress or temperature variation when yield surface is reached. On the other hand, TRIP results from internal stresses arising either from the volume change associated with the transformation or from the accompanying shape change without reaching the yield surface of the weaker phase involved (Leblond *et al.* 1989; Fischer *et al.* 2000).

TRIP phenomenon is usually associated with two distinct physical mechanisms, which have been proposed by Greenwood & Johnson (1965) and Magee (1966). The Greenwood-Johnson effect is due to an accommodation process of the microplasticity associated with a volume change. The Magee effect, on the other hand, is due to an orientation effect that arises from a shear internal stress state, which favors the thermodynamically preferred orientation direction for martensite formation in the presence of an external stress field, involving shape change.

Many efforts have been done towards for the TRIP modeling (Taleb *et al.* 2001; Homberg, 2004). The great majority of these models focus on micro scale features. Moreover, some of them discard the Magee effect for particular studies. Concerning TRIP effect on SMAs, it should be highlighted studies related to cyclic loading responses of SMAs

(Lagoudas *et al.* 2003; Auricchio *et al.* 2002; Chao *et al.* 2012). The main characteristic observed in the stress-strain curves during the training process are the reduction of the phase transformation stress and the increase of the residual permanent deformation which characterizes the TRIP effect (Auricchio *et al.* 2002). Lagoudas & Pavlin (2003) presented the modeling of the TRIP effect in SMAs while Entchev & Lagoudas (2003) discussed the TRIP model for porous SMAs.

This paper presents a three-dimensional constitutive model to describe both classical plasticity and transformation induced plasticity. The proposed model is an extension of the one presented by Oliveira *et al.* (2016, 2009) that is inspired on the one-dimensional model discussed in the following references: Paiva *et al.* (2005); Savi & Paiva (2005); Savi *et al.* (2002); Baeta-Neves *et al.* (2004). The goal of this work is to describe the macroscopic manifestation of the TRIP phenomenon on SMAs, exploring its influence on cyclic loadings. Numerical simulations are carried out establishing a comparison with experimental data showing the model's ability to capture TRIP phenomenon.

2. CONSTITUTIVE MODEL

The thermomechanical description of the TRIP effect in SMAs is based on the previous model presented in Oliveira *et al.* (2016, 2009). This model is developed within the framework of continuum mechanics and generalized standard materials approach (Lemaitre & Chaboche, 1990). Under this assumption, the thermomechanical behavior can be described by the Helmholtz free energy density, *Ψ*, and the pseudo-potential of dissipation, *Φ*. This approach assures that the second law of thermodynamics is satisfied, avoiding inconsistent behaviors. Based on that, the thermomechanical behavior of SMAs is described by the following set of equations.

$$\sigma_{ij} = E_{ijkl}\varepsilon_{kl} + \alpha\omega_{ij}\left(\beta^- - \beta^+\right) - \varOmega_{ij}\left(T - T_0\right)$$

$$\dot{\beta}^+ = \frac{1}{\eta^+}\left\{\varGamma\alpha + \varLambda + P - \alpha_{ij}^h\varOmega_{ij}\left(T - T_0\right) - \eta^I K\vartheta - \eta_{ij}^K\frac{\varsigma_{ij}}{H} - \tau^+\right\} + 7^+$$

$$\dot{\beta}^- = \frac{1}{\eta^-}\left\{-\varGamma\alpha + \varLambda - P + \alpha_{ij}^h\varOmega_{ij}\left(T - T_0\right) - \eta^I K\vartheta - \eta_{ij}^K\frac{\varsigma_{ij}}{H} - \tau^-\right\} + 7^-$$

$$\dot{\beta}^A = \frac{1}{\eta^A}\left\{P^A + \varLambda^{\aleph} + \varepsilon_{ij}^e\left(\varOmega_{ij}^A - \varOmega_{ij}^M\right)\left(T - T_0\right) - \frac{1}{2}\left(K^A - K^M\right)\vartheta^2 - \left(\frac{1}{2H^A} - \frac{1}{2H^M}\right)\varsigma_{ij}\varsigma_{ij} + \eta^I K\vartheta + \eta_{ij}^K\frac{\varsigma_{ij}}{H} - \tau^A\right\} + 7^A$$

$$\dot{\varepsilon}_{ij}^p = \gamma\frac{\hat{\sigma}_{ij} - \varsigma_{ij}}{\left\|\hat{\sigma}_{ij} - \varsigma_{ij}\right\|} \qquad \dot{\vartheta} = \sqrt{\frac{2}{3}}\gamma + \eta^I\left(\dot{\beta}^+ + \dot{\beta}^- + \dot{\beta}^A\right) \qquad \dot{\varsigma}_{ij} = \frac{2}{3}H\dot{\varepsilon}_{ij}^p + \eta_{ij}^K\left(\dot{\beta}^+ + \dot{\beta}^- + \dot{\beta}^A\right)$$

$$\dot{\varepsilon}_{ij}^{trip} = 2\sigma_{ij}\left\{\left(M_{13}\beta^+ + M_{31}\beta^A\right)\dot{\beta}^+ + \left(M_{32}\beta^- + M_{23}\beta^A\right)\dot{\beta}^- + \left[M_{43}\beta^A + M_{34}\left(1 - \beta^+ - \beta^- - \beta^A\right)\right]\dot{\beta}^A\right\}$$

$$\dot{\xi}^+ = \left|\dot{\beta}^+\right| \quad \dot{\xi}^- = \left|\dot{\beta}^-\right| \quad \dot{\xi}^A = \left|\dot{\beta}^A\right|$$

Yield surface and its conditions: $f = \left\|\hat{\sigma}_{ij} - \varsigma_{ij}\right\| - \sqrt{\frac{2}{3}}\left(\sigma_Y - K\vartheta\right)$; $\gamma \geq 0$, $f \leq 0$ and $\gamma f = 0$; $\gamma\dot{f} = 0$ if $f = 0$

This model considers four macroscopic phases: austenite (*A*), twinned martensite (*M*), which is stable in the absence of a stress field; and two phases associated with detwinned martensite, M^+ and M^-. In this regard, volume fraction of each phase should be considered: β^A is volume fraction of austenite (*A*); β^+ and β^-, are the volume fraction of martensitic variants (M^+ and M^-, respectively); the fourth phase is associated with twinned martensite (*M*) and its volume fraction is β^M. Since $\beta^M = 1 - \beta^+ - \beta^- - \beta^A$. In the previous equations, ε_{ij}^e, is the elastic strain; T is the temperature; T_0 is a reference temperature in a stress-free state; ϑ is the isotropic hardening variable; ς_{ij} is the kinematic hardening tensor; $\hat{\sigma}_{ij}$ is the deviatoric tensor of σ_{ij}. Finally, ξ^+, ξ^-, ξ^A are the new internal variables specifically related to the TRIP phenomenon.

Concerning parameters, subscript A and M are respectively related to austenitic and martensitic phases; α is a parameter that control the height of the stress-strain hysteresis loop; $\varLambda^M$ and $\varLambda^A$ are functions of temperature that define the phase transformation stress value; $\varOmega_{ij}$ is a tensor related to the thermal expansion coefficients; K it is the plastic modulus; H is the kinematical hardening modulus; ρ is the material density; $\eta^m (m = +, -, A)$ is associated with the internal dissipation of each material phase; η^I defines the coupling between phase transformation and isotropic hardening; η_{ij}^K is the second-order tensor associated with the kinematic hardening.

Internal constraints need to be considered in order to properly describe dissipation phenomena associated with phase transformation and plasticity. In this regard, indicator functions are defined to establish convex sets. τ is related to the sub-differential with respect to volume fractions being associated with projections in the β-space:

$$\tau = \left(\tau^+, \tau^-, \tau^A\right) \in \partial I_\pi\left(\beta^+, \beta^-, \beta^A\right) \tag{1}$$

where $I_\pi(\beta^+,\ \beta^-,\beta^A)$ is the indicator function associated with the convex π.

The set $\daleth$ is related to the sub-differential with respect to $\dot\beta^+,\dot\beta^-$ and $\dot\beta^A$.

$$\daleth = \left(\daleth^+,\daleth^-,\daleth^A\right) \in \partial I_\chi\left(\dot\beta^+,\dot\beta^-,\dot\beta^A\right) \tag{2}$$

where $I_\chi(\dot\beta^+,\ \dot\beta^-,\dot\beta^A)$ is the indicator function associated with the convex χ.

Besides, plasticity behavior is described using the classical approach considering that γ is the plastic multiplier; I_f is the indicator function related to the classical plasticity and σ_Y is the yield stress. Moreover, plastic behavior is subjected to the Kuhn-Tucker conditions $\gamma \geq 0, f \leq 0$ and $\gamma f = 0$ and the consistency condition $\gamma \dot f = 0$ if $f = 0$.

The use of a limit number of martensitic variants is possible due to the definition of an equivalent strain field, Γ, which induces phase transformations (Oliveira *et al*. 2016). The definition of this equivalent strain field Γ is based on experimental observations that show that both volumetric and deviatoric effects induce the phase transformations with the same qualitative behavior. Its definition is as follows:

$$\Gamma = \frac{1}{3}\varepsilon_{kk}^e + \frac{2}{3}\sqrt{3J_2^e}\,\mathrm{sign}\left(\varepsilon_{kk}^e\right) \tag{3}$$

Note that this strain filed has volumetric and deviatoric terms that are respectively given by:

$$\varepsilon_{kk}^e = \varepsilon_{11}^e + \varepsilon_{22}^e + \varepsilon_{33}^e \tag{4}$$

$$J_2^e = \frac{1}{6}\hat\varepsilon_{ij}^e\hat\varepsilon_{ij}^e = \frac{1}{6}\left\{\left(\varepsilon_{11}^e - \varepsilon_{22}^e\right)^2 + \left(\varepsilon_{22}^e - \varepsilon_{33}^e\right)^2 + \left(\varepsilon_{33}^e - \varepsilon_{11}^e\right)^2 + 6\left[\left(\varepsilon_{12}^e\right)^2 + \left(\varepsilon_{13}^e\right)^2 + \left(\varepsilon_{23}^e\right)^2\right]\right\} \tag{5}$$

where the deviatoric elastic strain is given by

$$\hat\varepsilon_{ij}^e = \varepsilon_{ij}^e - \frac{1}{3}\varepsilon_{kk}^e\delta_{ij} \tag{6}$$

and

$$\mathrm{sign}\left(\varepsilon_{kk}^e\right) = \begin{cases} +1, \text{ if } \varepsilon_{kk}^e \geq 0 \\ -1, \text{ if } \varepsilon_{kk}^e < 0 \end{cases} \tag{7}$$

An additive composition is assumed including a new TRIP strain term:

$$\varepsilon_{ij}^e = \varepsilon_{ij} - \varepsilon_{ij}^p - \varepsilon_{ij}^t - \varepsilon_{ij}^{trip} \tag{8}$$

The phase transformation strain defines the width of the stress-strain hysteresis loop, being written as follows:

$$\varepsilon_{ij}^t = \alpha_{ijkl}^h r_{kl}\left(\beta^+ - \beta^-\right)\mathrm{sign}\left(\varepsilon_{kk}^e\right) \tag{9}$$

where α_{ijkl}^h is a fourth-order tensor related to phase transformations that considers different parameters for normal and shear behaviors. Its form is similar to the classical isotropic elastic tensor (Oliveira *et al*. 2016).

$$\alpha_{ijkl}^h = \begin{bmatrix} \alpha_N^h & \alpha_N^h - \alpha_S^h & \alpha_N^h - \alpha_S^h & 0 & 0 & 0 \\ \alpha_N^h - \alpha_S^h & \alpha_N^h & \alpha_N^h - \alpha_S^h & 0 & 0 & 0 \\ \alpha_N^h - \alpha_S^h & \alpha_N^h - \alpha_S^h & \alpha_N^h & 0 & 0 & 0 \\ 0 & 0 & 0 & \alpha_S^h & 0 & 0 \\ 0 & 0 & 0 & 0 & \alpha_S^h & 0 \\ 0 & 0 & 0 & 0 & 0 & \alpha_S^h \end{bmatrix} \tag{10}$$

where α_N^h is the normal component and α_S^h is the shear component of α_{ijkl}^h.

The definition of transformation strain, ε_{ij}^t, needs the definition of parameter r_{kl} that is a symmetric second-order tensor related to the loading history (Oliveira *et al*. 2016) as follows:

$$r_{kl} = \begin{cases} +1, & \text{if} \quad \sigma_{kl} > 0 \\ 0, & \text{if} \quad \sigma_{kl} = 0 \\ -1, & \text{if} \quad \sigma_{kl} < 0 \end{cases} \tag{11}$$

For situations where mechanical loadings are provided by multiaxial, non-simultaneous load history, tensor r_{kl} is evaluated as follows for the subsequent loadings:

$$r_{kl} = \frac{\sigma_{kl}}{\left|S_{kl}^{max}\right|} \quad \text{if } \beta^+ \neq 0 \quad \text{or } \beta^- \neq 0 \tag{12}$$

where S_{kl}^{max} represents the maximum value of the mechanical loading that can be a stress or a strain. Besides, note that $\frac{S_{kl}^{max}}{|S_{kl}^{max}|} = 0$ if $S_{kl}^{max} = 0$.

Moreover, auxiliary quantities are defined as follows:

$$\omega_{ij} = \frac{1}{3}\delta_{ij} + \left[\frac{3\varepsilon_{ij}^e - \varepsilon_{kk}^e \delta_{ij}}{3\sqrt{3J_2^e}}\right] \text{sign}\left(\varepsilon_{kk}^e\right) \tag{13}$$

$$P = \left(\lambda \varepsilon_{kk}^e \alpha_{ijkl}^h r_{kl} \delta_{ij} + 2\mu \varepsilon_{ij}^e \alpha_{ijkl}^h r_{kl}\right) + \alpha\left(\beta^- - \beta^+\right)\left\{\frac{1}{3}\alpha_{ijkl}^h r_{kl}\delta_{ij} + \frac{2P^\alpha}{\sqrt{3J_2^e}} \text{sign}\left(\varepsilon_{kk}^e\right)\right\} \tag{14}$$

$$P^A = -\frac{1}{2}\left(\lambda^A \left(\varepsilon_{kk}^e\right)^2 + 2\mu^A \varepsilon_{ij}^e \varepsilon_{ij}^e\right) + \frac{1}{2}\left(\lambda^M \left(\varepsilon_{kk}^e\right)^2 + 2\mu^M \varepsilon_{ij}^e \varepsilon_{ij}^e\right) \tag{15}$$

$$P^\alpha = \frac{(\alpha_S^h)}{6}\left\{(r_{11} - r_{22})(\varepsilon_{11}^e - \varepsilon_{22}^e) + (r_{22} - r_{33})(\varepsilon_{22}^e - \varepsilon_{33}^e) + (r_{33} - r_{11})(\varepsilon_{33}^e - \varepsilon_{11}^e) + 6(r_{12}\varepsilon_{12}^e + r_{13}\varepsilon_{13}^e + r_{23}\varepsilon_{23}^e\right\} \tag{16}$$

$$E_{ijkl}\varepsilon_{kl} = \lambda \varepsilon_{kk}^e \delta_{ij} + 2\mu \varepsilon_{ij}^e \tag{17}$$

where λ and μ are the Lamé coefficients; δ_{ij} is the Kronecker delta.

The coupling with the kinematic hardening is defined by the second-order tensor η_{ij}^K defined as follows:

$$\eta_{ij}^k = \eta^k \begin{bmatrix} 1 & 1 & 1 \\ 1 & 1 & 1 \\ 1 & 1 & 1 \end{bmatrix} \tag{18}$$

It is important to highlight that some constants are split due to temperature or loading dependence. In this regard, some changes can be used to facilitate adjustments with experimental data. Yield surface can be defined as a function of temperature. Besides, it is important to define the form of the temperature dependent phase transformation stress levels. The dissipation aspects of phase transformation may be defined using different parameters during loading and unloading. Therefore, it is important to define the details of some parameters.

Initially, consider the temperature dependent functions $\Lambda = \Lambda(T)$ and $\Lambda^\aleph = \Lambda^\aleph(T)$. The following definitions are adopted:

$$\Lambda = 2\Lambda^M = \begin{cases} -L_0^\pm + \frac{L^\pm}{T^M}\left(T - T^M\right) & \text{if } T > T^M \\ -L_0^\pm & \text{if } T > T^M \end{cases} \tag{19}$$

$$\Lambda^\aleph = \Lambda^M + \Lambda^A = \begin{cases} -L_0^A + \frac{L^A}{T^M}\left(T - T^M\right) & \text{if } T > T^M \\ -L_0^A & \text{if } T > T^M \end{cases} \tag{20}$$

where T^M is the temperature below which the martensitic phase becomes stable; note that the phase transformation stress level is constant for $T<T^M$.

The phase transformation dissipation can be defined contemplating the different characteristics of the phase transformation kinetics during loading and unloading processes. Therefore, different values can be employed for the parameters η and η^A, in the follow form: $\eta = \eta_L$ if $\dot{\Gamma} > 0$; $\eta = \eta_U$ if $\dot{\Gamma} < 0$; $\eta^A = \eta_L^A$ if $\dot{\Gamma} > 0$; $\eta^A = \eta_U^A$ if $\dot{\Gamma} < 0$. The parameters η_L, η_U, η_L^A and η_U^A are calculated considering fourth-order tensors, in the same way of the Equations (21) and (22).

$$\begin{cases} (\ ) = r_{ij} \widetilde{(\ )}_{ijkl} r_{kl} & \text{if } \Gamma^{\sigma} \neq 0 \\ (\ ) = (\ )_N & \text{otherwise} \end{cases} \tag{21}$$

where:

$$\widetilde{(\ )}_{ijkl} = \begin{bmatrix} (\ )_N & (\ )_N - (\ )_S & (\ )_N - (\ )_S & 0 & 0 & 0 \\ (\ )_N - (\ )_S & (\ )_N & (\ )_N - (\ )_S & 0 & 0 & 0 \\ (\ )_N - (\ )_S & (\ )_N - (\ )_S & (\ )_N & 0 & 0 & 0 \\ 0 & 0 & 0 & 2(\ )_S & 0 & 0 \\ 0 & 0 & 0 & 0 & 2(\ )_S & 0 \\ 0 & 0 & 0 & 0 & 0 & 2(\ )_S \end{bmatrix} \tag{22}$$

where $(\ \ )_N$ and $(\ \ )_S$ respectively represents the normal and the shear components; Γ^{σ} is the equivalent stress field, similar to the strain field Γ.

2.1. Saturation Parameters

In order to describe the TRIP effect, it is necessary to represent the saturation effect. This behavior is taken into account with exponential functions, associated the variables ξ^n related TRIP effect.

The parameters α, L_0^+, L_0^-, L^+, L^-, L_0^A , L^A, are presented in the general form:

$$\begin{cases} (\ ) = \widehat{(\ )} \left[\dfrac{N + \exp\left(-m^{(\ )} \xi^+\right)}{N+1} \right] \text{if } \Gamma \geq 0 \\ (\ ) = \widehat{(\ )} \left[\dfrac{N + \exp\left(-m^{(\ )} \xi^-\right)}{N+1} \right] \text{if } \Gamma < 0 \end{cases} \tag{23}$$

where ( ) represents the actual value of the parameter, $\widehat{(\ )}$ represents the nominal parameter value and $m^{(\ )}$ controls the saturation effect.

In addition, TRIP parameters are defined as follows:

$$M_{13} = \hat{M}_{13} \exp\left(-m^M \xi^+\right) \qquad M_{31} = \hat{M}_{31} \exp\left(-m^M \xi^+\right) \tag{24}$$

$$M_{23} = \hat{M}_{23} \exp\left(-m^M \xi^-\right) \qquad M_{32} = \hat{M}_{32} \exp\left(-m^M \xi^-\right) \tag{25}$$

$$M_{34} = \hat{M}_{34} \exp\left(-m^M \xi^A\right) \qquad M_{43} = \hat{M}_{43} \exp\left(-m^M \xi^A\right) \tag{26}$$

where m^M controls the saturation effect. Temperature dependence is considered assuming that parameters can have a linear dependence as shown in the following expression:

$$\widehat{M}_{13} = \begin{cases} 0 & \text{if } T < T^{trip} \\ \hat{M}_{13}^R \dfrac{\left(T - T^{trip}\right)}{\left(T^F - T^{trip}\right)} & \text{if } T \geq T^{trip} \end{cases} \tag{27}$$

where $\widehat{M}_{13}^R$ is a reference value of $\widehat{M}_{13}$ at $T = T^{trip}$ and T^{trip} is a temperature below which TRIP does not exist. Analogous expressions are used to M_{31}, M_{23} and M_{32}. For simplicity, this work considers M_{34}=M_{43} = 0.

3. NUMERICAL SIMULATIONS – UNIAXIAL TESTS

Numerical simulations are carried out in order to show the model capabilities to describe themomechancial behavior of SMAs. This section considers uniaxial tests by assuming that mechanical loading linearly varies from zero to a maximum value and then back to zero. Stress driving case is assumed. Table 1 presents constitutive parameters. Experimental results from Tobushi *et al.* (1991) are considered as a reference. In order to compare with the one-dimensional model, Poisson's ratio is vanished.

Initially, numerical simulations are compared with experimental data obtained by Tobushi *et al*. (1991). Figure 1 presents tests for three different temperatures: T=373K, T=353K and T=333K. It is noticeable a pseudoelastic behavior and that the model captures the general thermomechanical behavior, including the TRIP effect represented by a residual strain when the loading cycle is finished. This behavior, however, is temperature dependent. The higher temperature is related to higher value of the residual strain related to the TRIP effect.

Table 1- Parameters obtained from the experimental results obtained by Tobushi *et al.* (1991).

E^A(GPa)	E^M(GPa)	Ω^A(MPa/K)	Ω^M (MPa/K)	α_N^h(MPa)	α_S^h(MPa)
54	42	0.74	0.17	0.0453	0.0228
α(MPa)	$L_0^{\pm}$(MPa)	$L^{\pm}$ (MPa)	L_0^A(MPa)	L^A (MPa)	T^M (K)
330	0.15	41.5	0.63	180	291.4
T^F (K)	T^0(K)	$T^{trip}(K)$	σ_Y^M (GPa)	σ_Y^{Ai} (GPa)	σ_Y^{Af} (GPa)
423	307	333	1	3	2
K^A(GPa)	K^M(GPa)	H^A(GPa)	H^M (GPa)	η^I	η^K
1.4	0.4	4	1.1	-0.01	-0.01
$(\eta_L)_N$ (MPa.s)	$(\eta_U)_N$(MPa.s)	$(\eta_L^A)_N$ (MPa.s)	$(\eta_U^A)_N$(MPa.s)	$(\eta_L)_S$ (MPa.s)	$(\eta_U)_S$(MPa.s)
1	2.4	1	2.4	1	2.4
$(\eta_L^A)_S$ (MPa.s)	$(\eta_U^A)_S$(MPa.s)	$\widehat{M}_{13}$ (GPa^{-1})	$\widehat{M}_{31}$(GPa^{-1})	$\widehat{M}_{23}$ (GPa^{-1})	$\widehat{M}_{32}$(GPa^{-1})
1	2.4	0.009	0.009	0.009	0.009
m^α	m^L	m^M	N	υ^A	υ^M
0.2	0.1	0.1	2	0.40	0.42

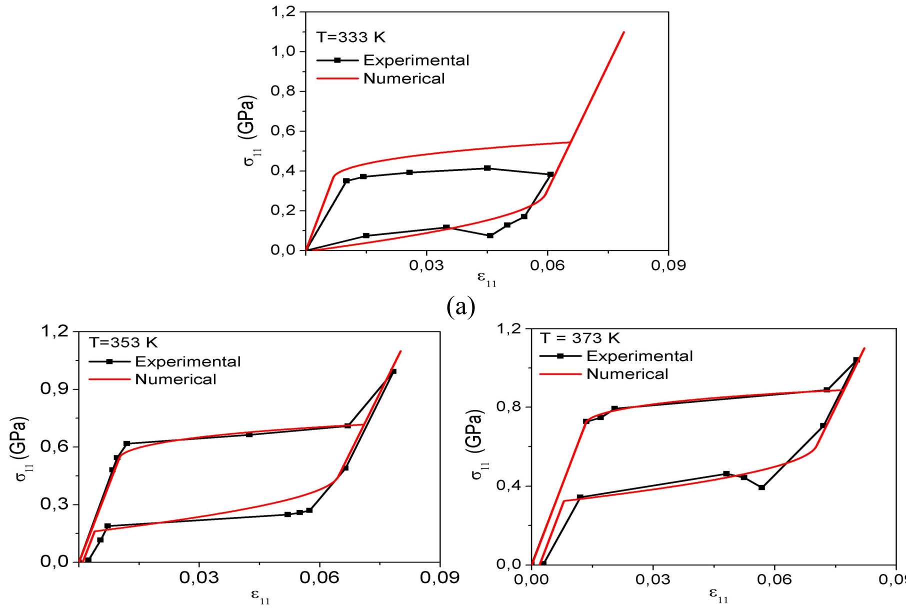

(a) (b) (c)

Figure 1- Numerical-experimental comparison: (a) T=333K; (b) T=353K; (c) T=373K.

The TRIP effect has a saturation characteristic meaning that its influence reduces when the number of cycles increases. Because of that, SMA actuators need to be subjected to training process that eliminates the influence of this phenomenon. Figure 2 presents results of a cyclic response of an SMA sample (Lagoudas *et al*. 2003) compared with numerical simulations related to the same experimental data. Table 2 presents model parameters employed for simulations. Figure 2(a) shows stress-strain curves establishing a comparison between experimental and numerical results. Figure 2(b) presents phase transformation evolution showing volume fraction time history. Figure 2(c) shows the evolution of the TRIP effect. After the first fifteen cycles, the TRIP strain assumes a constant value, stabilizing the hysteresis loop. Note that this kind of simulation can be performed in order to evaluate the number of cycles needed for a proper training process.

Table 2- Model parameters that match experimental results due to Lagoudas *et al.* (2003).

E^A(GPa)	E^M(GPa)	Ω^A(MPa/K)	Ω^M (MPa/K)	α_N^h(MPa)	α (MPa)
72	28.2	0.74	0.17	0.037	140
$L_0^{\pm}$(MPa)	$L^{\pm}$ (MPa)	L_0^A(MPa)	L^A (MPa)	T^M (K)	T^F (K)
0.1	41.5	0.63	147	291.4	423
T^0(K)	T^{trip} (K)	σ_Y^M (GPa)	σ_Y^{Ai} (GPa)	σ_Y^{Af} (GPa)	K^A(GPa)
307	330	5	15	10	1.4
K^M(GPa)	H^A(GPa)	H^M (GPa)	η^I	η^K	$(\eta_L)_N$ (MPa. s)
0.4	4	1.1	-0.01	-0.01	0.1
$(\eta_U)_N$(MPa.s)	$(\eta_L^A)_N$ (MPa. s)	$(\eta_U^A)_N$(MPa.s)	$\hat{M}_{13}$ (GPa^{-1})	$\hat{M}_{31}$(GPa^{-1})	m^α
0.04	0.1	0.04	0.072	0.071	0.07
m^L	m^M	N	υ^A	υ^M	
0.2	0.14	2	0	0	

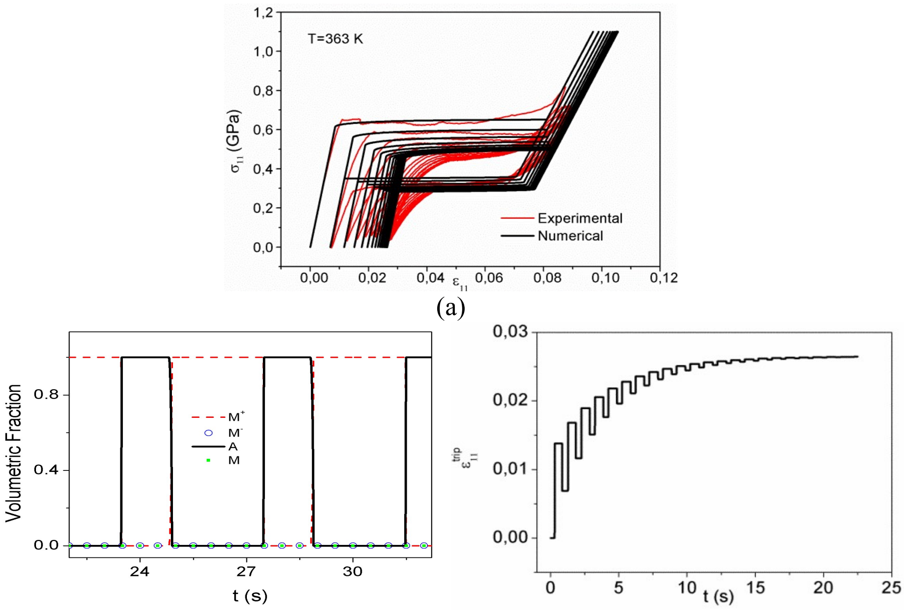

(a)

(b) (c)

Figure 2- Cyclic loading test: (a) stress-strain curves; (b) volume fractions; (c) TRIP strain evolution.

4. NUMERICAL SIMULATIONS – MULTIAXIAL TESTS

This section investigates SMAs subjected to multiaxial tests. Initially, a pure shear test is carried out showing the coordinate invariance of the model. Afterward, the pure shear test with plasticity is treated. Finally, a tension-torsion coupled test is carried out, showing the influence of TRIP effect in this three-dimensional test.

4.1. Pure ShearTest

This section analyzes the pure shear test. The main idea is to compare the pure shear test with its analogous tension-compression test. A situation where the SMA specimen reaches the yield surface is in focus, presenting plastic behavior. Stress driving case is assumed with the maximum stress components as follows. Table 1 presents model parameters employed for simulations.

$$\sigma^{Shear} = \begin{bmatrix} 0 & 0.85 & 0 \\ 0.85 & 0 & 0 \\ 0 & 0 & 0 \end{bmatrix} \text{GPa} \qquad \sigma^{Equivalent} = \begin{bmatrix} 0.85 & 0 & 0 \\ 0 & -0.85 & 0 \\ 0 & 0 & 0 \end{bmatrix} \text{GPa}$$

Figure 3 presents the SMA response for both pure shear and tension-compression tests. Figure 3(a) presents stress-strain curves comparing both equivalent loading process, showing that both curves are identical. Figure 3(b) presents volume fraction evolutions while Figure 3(c) presents TRIP strain and plastic strain evolutions.

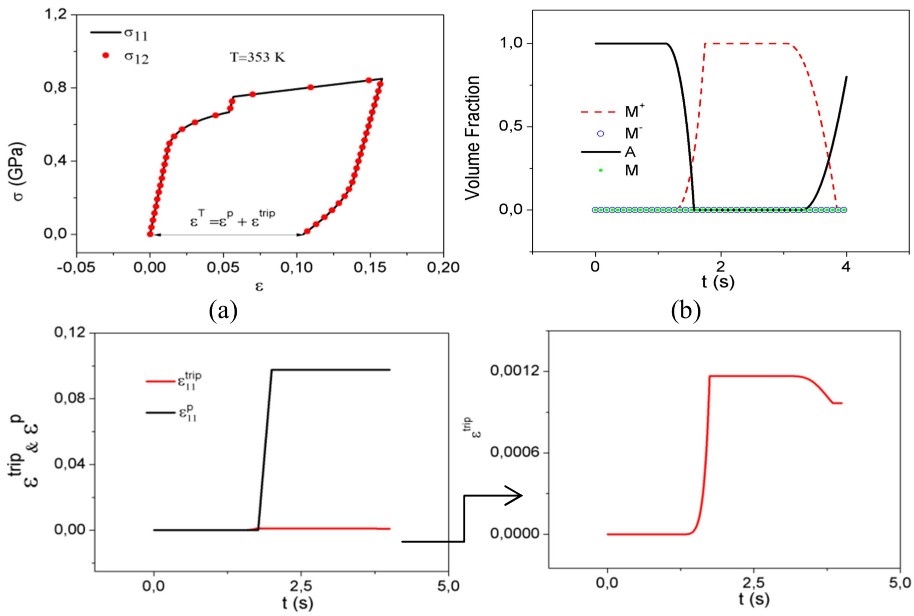

(a) (b) (c)

Figure 3 - Pure shear test with plasticity. (a) Stress-strain curves; (b) volume fraction evolution; (c) plastic and TRIP strain evolutions.

4.1.1. Coupled Tension-Torsion Test

This section deals with a coupled tension-torsion test. Figure 4 presents results for uncoupled test considering tension and torsion tests without TRIP, employed to adjust model parameters presented in Table 3.

Table 3- Model parameters used to coupled tension-torsion test.

E^A(GPa)	E^M(GPa)	Ω^A(MPa/K)	Ω^M (MPa/K)	α_N^h(MPa)	α_S^h(MPa)
65	29	0.74	0.17	0.0148	0.0176
α(MPa)	$L_0^{\pm}$(MPa)	$L^{\pm}$ (MPa)	L_0^A(MPa)	L^A (MPa)	T^M(K)
1	0.6	5	3.5	30	223
T^F(K)	T^0(K)	T^{trip}(K)	σ_Y^M (GPa)	σ_Y^{Ai} (GPa)	σ_Y^{Af} (GPa)
423	285	270	0.5	1.5	1
K^A(GPa)	K^M(GPa)	H^A(GPa)	H^M (GPa)	η^I	η^K
1.4	0.4	4	1.1	-0.01	-0.01
$(\eta_L)_N$ (MPa. s)	$(\eta_U)_N$(MPa.s)	$(\eta_L^A)_N$ (MPa. s)	$(\eta_U^A)_N$(MPa.s)	$(\eta_L)_S$ (MPa. s)	$(\eta_U)_S$(MPa.s)
2.3	1	15	0.88	1.9	2.8
$(\eta_L^A)_S$ (MPa. s)	$(\eta_U^A)_S$(MPa.s)	$\widehat{M}_{13}$ (GPa^{-1})	$\widehat{M}_{31}$(GPa^{-1})	$\widehat{M}_{23}$ (GPa^{-1})	$\widehat{M}_{32}$(GPa^{-1})
3	0.8	0.05	0.05	0.05	0.05
m^α	m^L	m^M	N	υ^A	υ^M
0.1	0.4	0.2	2	0.36	0.36

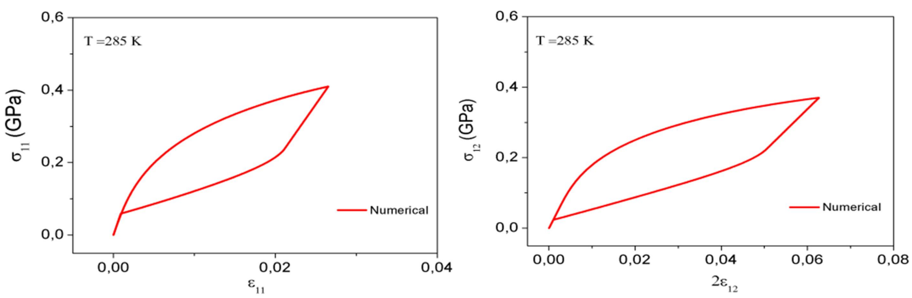

(a) (b)

Figure 4 - Response for tensile test and shear test. (a) $\sigma_{11} \times \varepsilon_{11}$, (b) $\sigma_{12} \times 2\varepsilon_{12}$.

Figure 5 presents the loading process and SMA response. Note that loading process considers different mechanical loadings involving tension and torsion. Results are presented as stress-strain curves and tension-torsion strain curves. In addition, the evolution of TRIP and plastic strains are also shown. Note that TRIP phenomenon is observed presenting the expected stabilization behavior.

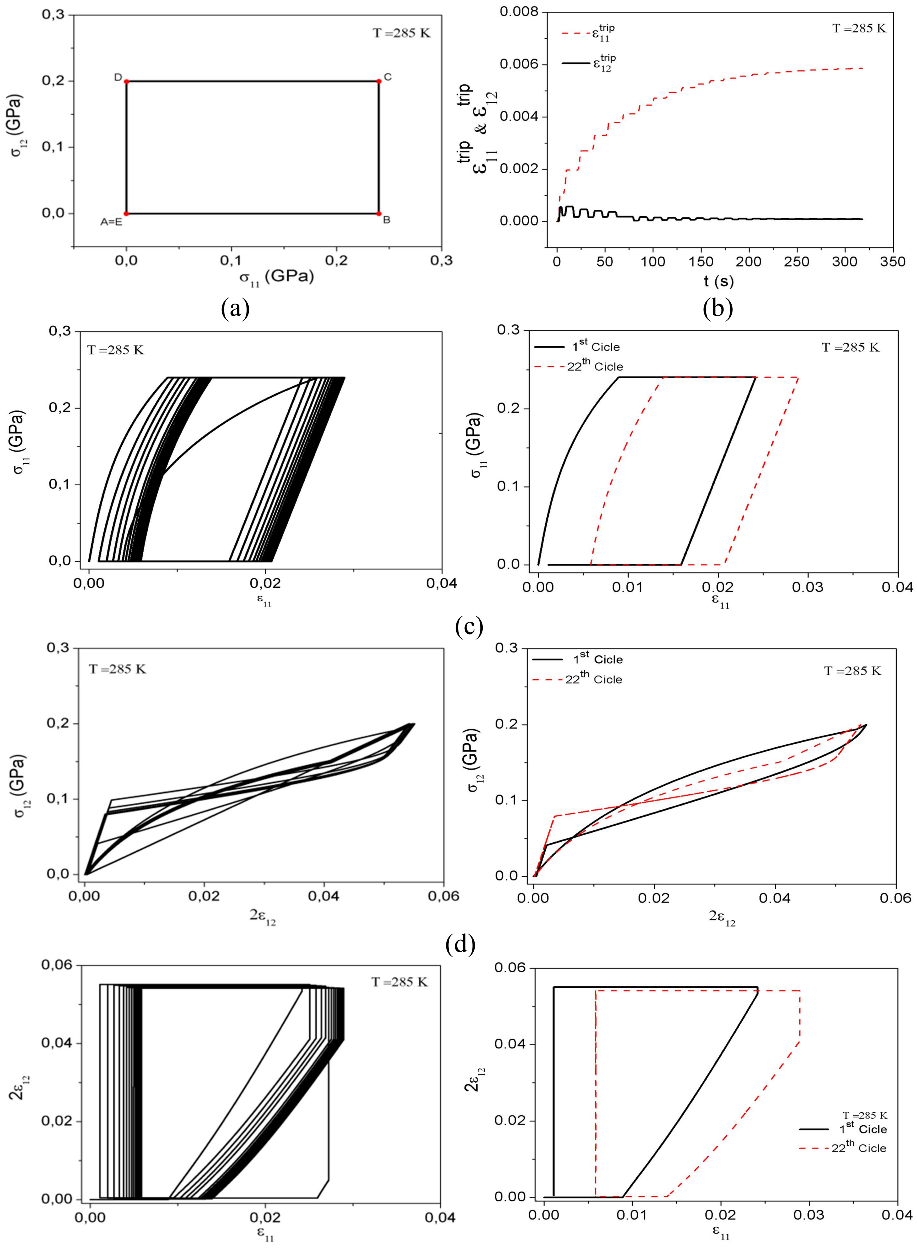

Figure 5 - Tension-torsion test. (a) Loading process of the coupled tension-shear test; (b) time history of ε_{11}^{trip} and ε_{12}^{trip}; (c) $\sigma_{11} \times \varepsilon_{11}$; (d) $\sigma_{12} \times 2\varepsilon_{12}$; (e) $2\varepsilon_{12} \times \varepsilon_{11}$.

5. CONCLUSIONS

This work presents a three-dimensional model to describe the transformation induced plasticity on shape memory alloys. Essentially, the constitutive model proposed by Oliveira *et al.* (2016) is extended considering new state variables associated with the TRIP effect. Model parameters are described by exponential functions in order to represent the saturation effect. Numerical simulations are carried out for uniaxial and multiaxial tests. Concerning uniaxial tests, results are in close agreement with experimental data presented in Tobushi *et al.* (1991) for tensile tests and Lagoudas *et al.* (2003) for cyclic loading test. Multiaxial tests consider pure shear test showing the material invariance with an equivalent tension-compression test. Moreover, a coupled tension-torsion test is treated showing the capacity of the model to describe TRIP effect.

6. ACKNOWLEDGEMENTS

The authors would like to acknowledge the support of the Brazilian Research Agencies CNPq, CAPES and FAPERJ and through the INCT-EIE (National Institute of Science and Technology - Smart Structures in Engineering) the CNPq and FAPEMIG. The Air Force Office of Scientific Research (AFOSR) is also acknowledged.

7. REFERENCES

Auricchio F., Marfia S., Sacco E., 2002, "Modeling of SMA Materials: Training and Two Way Memory Effects", Computers and Structures, v. 81, n. 24, pp. 2301-2317.

Baêta-Neves, A.P., Savi, M.A., Pacheco, P.M.C.L., 2004, "On the Fremond's Constitutive Model for Shape Memory Alloys", Mechanics Research Communication, v. 31, n. 6, pp. 677-688.

Entchev, P.B., Lagoudas, D.C., 2004, "Modeling of transformation-induced plasticity and its effect on the behavior of porous shape memory alloys. Part II: porous SMA response", Mechanics of materials, v. 36, n. 9, pp. 893-913.

Fischer, F.D., Reisner, G., Werner, E., Tanaka, K., Cailletaud, G. &Antretter, T., 2000, "A New View on Transformation Induced Plasticity", International Journal of Plasticity, v. 16, n. 7, pp. 723-748.

Gautier, E., Zhang, X.M. & Simon, A., 1989, "Role of Internal Stress State on Transformation Induced Plasticity and Transformation Mechanisms during the Progress of Stress Induced Phase Transformation", International Conference on Residual Stresses – ICRS2, (Ed: G. Beck, S. Denis and A. Simon), Elsevier Applied Science, London, pp. 777-783.

Gautier, E., 1998, "Déformation de transformation et plasticité de transformation", École d'été MH2M, Méthodes d'Homogénéisationen Mécanique des Matériaux, La Londe Les Maures (Var, France).

Greenwood, G.W. & Johnson, R.H., 1965, "The Deformation of Metals under Small Stresses during Phase Transformation", Proceedings of the Royal Society, v. 283, n. 1394, pp. 403-422.

Lagoudas, D.C., Entchev, P.B. & Kumar, P.K., 2003, "Thermomechanical Characterization SMA Actuators Under Cyclic Loading", Proceedings of IMECE'03, ASME International Mechanical Engineering Congress.

Lagoudas, D.C., 2008, "Shape Memory Alloys, Modeling and Engineering Applications", Department of Aerospace Engineering Texas A&M University, Springer Science Business Media, LLC.

Lagoudas, D.C., Entchev, P.B., 2004, "Modeling of transformation-induced plasticity and its effect on the behavior of porous shape memory alloys. Part I: constitutive model for fully dense SMAs". Mechanics of Materials, v. 36, n. 9, pp. 865-892.

Leblond, J.B., 1989, "Mathematical Modeling of Transformation Plasticity in Steels II: Coupling with Strain Hardening Phenomena", International Journal of Plasticity, v. 5, n. 6, pp. 573-591.

Leblond, J.B., Devaux, J., Devaux, J.C., 1989, "Mathematical Modeling of Transformation Plasticity in Steels I: Case of Ideal-Plastic Phases", International Journal of Plasticity; v. 5, n. 6, pp.551-572.

Lemaitre, J., Charboche, J.L., 1990, "Mechanics of Solid Materials", Cambridge University Press.

Magge, C.L., 1996, "Transformation Kinetics, Microplasticity and Aging of Martensite in Fe-31 Ni", PhD, Thesis, Carnegie Institute of Technology, Pittsburg, PA.

Oliveira, S.A., Savi, M.A., Kalamkarov A.L., 2010, "A Three-Dimensional Constitutive Model for Shape Memory Alloys", Archive of Applied Mechanics, v. 80, n.10, pp. 1163-1175.

Oliveira, S.A., Savi, M.A., Zouain, N., 2016, "A Three-Dimensional Description of Shape Memory Alloy Thermomechanical Behavior Including Plasticity", Journal of the Brazilian Society of Mechanical Sciences and Engineering, v.38, n.5, pp.1451-1472.

Paiva, A., Savi, M.A., 2006, "An Overview of Constitutive Models for Shape Memory Alloys", Mathematical Problems in Engineering, v.2006, Article ID56876, pp.1-30.

Paiva, A., Savi, M.A., Braga, A.M.B. & Pacheco, P.M.C.L., 2005b, "A Constitutive Model for Shape Memory Alloys Considering Tensile-Compressive Asymmetry and Plasticity", International Journal of Solids and Structures, v.42, n.11-12, pp.3439-3457.

Piecyska, E., Gadaj, S., Nowacki, W.K., Hoshio, K., Machino, Y., Tobushi, H., 2005, "Characteristics of Energy Storage and Dissipation in TiNi Shape Memory Alloys", Science and Technology of Advanced Materials, v. 6, n. 8, pp. 889-894.

Savi, M.A., Paiva, A., 2005, "Describing Internal Subloops Due to Incomplete Phase Transformations in Shape Memory Alloys", Archive of Applied Mechanics, v. 74, n. 9, pp.637-647.

Savi, M.A., Paiva A., Baeta-Neves, A.P., Pacheco, P.M.C.L., 2002, "Phenomenological Modeling and Numerical Simulation of Shape memory: A Thermo-Plastic Phase Transformation Coupled Model", Journal of Intelligent Materials Systems and Structures, v. 3, n. 5, pp. 261-273.

Stringfellow, R.G., Parks, D.M. & Olson, G.B., 1992, "A Constitutive Model for Transformation Plasticity Accompanying Strain-induced Martensitic Transformation in Metastable Austenitic Steels", ACTA Metallurgical, v. 40, n. 7, pp. 1703-1716.

Taleb, L., Cavallo, N. &Waeckel, F., 2001, "Experimental Analysis of Transformation Plasticity", International Journal of Plasticity, v 17, n. 1, pp. 1-20.